Increased level of FAM19A5 is associated with cerebral small vessel disease and leads to a better outcome

Zhongnan Hao, Shaonan Yang, Ruihua Yin, Jin Wei, Yuan Wang, Xudong Pan and Aijun Ma

The Affiliated Hospital of Qingdao University, Qingdao, China

ABSTRACT

Objective. FAM19A5 plays an essential role in the development and acute or chronic inflammation of the central nervous system. The present study aimed to explore the association between FAM19A5 and cerebral small vessel disease (cSVD).

Methods. A total of 344 recent small subcortical infarct (RSSI) patients and 265 healthy controls were included in this study. The difference in the FAM19A5 level between the two groups was compared and the correlation between FAM19A5 and cerebral infarction volume was analyzed. Also, the association between FAM19A5 and the total magnetic resonance imaging (MRI) burden with its imaging characteristics was explored. Moreover, the correspondence of FAM19A5 with the outcome was assessed via Δ National Institutes of Health Stroke Scale score (NIHSS) and the percentage of NIHSS improvement.

Results. FAM19A5 was highly expressed in the RSSI group ($P = 0.023$), showing a positive correlation with cerebral infarction volume ($P < 0.01$). It was positively correlated with total MRI cSVD burden ($P < 0.001$) and reflected the severity of white matter hyperintensity (WMH) ($P < 0.01$) and enlarged perivascular space (EPVS) ($P < 0.01$), but did not show any association with cerebral microbleed (CMB) and lacune. Moreover, FAM19A5 suggested a larger Δ NIHSS ($P = 0.021$) and NIHSS improvement percentage ($P = 0.007$).

Conclusion. Serum FAM19A5 was increased in RSSI and positively correlated with the infarct volume. It also reflects the total MRI burden of cSVD, of which the imaging characteristics are positively correlated with WMH and EPVS. In addition, higher FAM19A5 levels reflect better outcomes in RSSI patients.

INTRODUCTION

Recent small subcortical infarction (RSSI), formerly known as lacunar infarct, accounts for 25% of all acute ischemic strokes. It results from the occlusion of a minor, single perforating brain artery, supplying subcortical areas in the deep white matter, basal ganglia (BG), thalamus, or pons (*Cannistraro et al., 2019*; *Gattringer et al., 2015*). Typically, the core mechanism of cSVD-related brain acute injury is considered to be ischemia, which effectuates through arteriolar stenosis or occlusion, irrespective of structural or

functional (such as vasospasm, impaired self-regulation, or hypotension) (*Wardlaw, Smith & Dichgans, 2013a*). RSSI is one of the critical MRI characteristics of cerebral small vessel disease (cSVD). Lacune, white matter hyperintensity (WMH), enlarged perivascular space (EPVS), and cerebral microbleed (CMB) are also components of cSVD imaging characteristics (*Wardlaw et al., 2013b*). The main symptoms of cSVD are stroke (subcortical infarction and cerebral hemorrhage), cognitive and affective disorders, gait disorder, and overall function decline. The pathogenesis of cSVD is complicated; various MRI imaging characteristics and different parts of lesion sites show unique pathogenesis that is independent and interrelated (*Blanco, Müller & Spence, 2017*; *Satizabal et al., 2012*; *Wardlaw, Smith & Dichgans, 2013a*).

FAM19A5, also known as TAFA-5, belongs to the family with sequence similarity 19 comprising five highly homologous genes (*FAM19A1-5*) (*Tom Tang et al., 2004*). Using X-gal staining in FAM19A5-LacZ knock-in mice, a previous found that FAM19A5 participates in the nervous system development from an early stage, expresses in neurons, oligodendrocyte precursor cells (OPCs), astrocytes, and microglia. Also, using the traumatic brain injury (TBI) model, FAM19A5 is suggested to be involved in the OPC-mediated repair process as an acute inflammatory factor after pathological brain injury (*Shahapal et al., 2019*). The participation of FAM19A5 in the TNF-α-induced hypothalamus inflammatory response also confirmed the role of FAM19A5 in acute inflammation (*Kang et al., 2020*). Moreover, as a bridge connecting chronic inflammation, reactive gliosis, and degenerative diseases in the brain, FAM19A5 is overexpressed in severe depressive disorder, Alzheimer's, Parkinson's disease, and vascular dementia (*Han et al., 2020*; *Li et al., 2020*; *Li et al., 2021*; *Mez et al., 2017*).

Several studies demonstrated that inflammation plays a crucial role in the pathogenesis of cSVD (*Blanco, Müller & Spence, 2017*; *Kwee & Kwee, 2007*; *Satizabal et al., 2012*; *Wardlaw, Smith & Dichgans, 2013a*); whether FAM19A5 affects the pathogenesis of cSVD as an inflammatory factor has not yet been published. Based on the association among laboratory, imaging, and clinical assessments, the present study aimed to explore the correlation between FAM19A5 and cSVD.

METHODS

Subjects

Cerebral infarction patients and healthy individuals admitted to the Institute of Cerebrovascular Diseases Cooperative Medical Institutions from May 2018 to June 2020 were continuously enrolled in this study. RSSI is defined as a recent deep small infarction caused by a single perforating artery occlusion, leading to ischemic necrosis of the brain tissue in its blood supply area. The inclusion criteria were as follows: RSSI patients showing typical cerebral infarction symptoms and physical signs with ischemic focus <20 mm in brain MRI. The exclusion criteria were as follows: patients with carotid or intracranial artery stenosis >50%, cardiogenic stroke, previous cardiocerebrovascular disease, severe liver or kidney function injury, and inflammation-related diseases, such as rheumatic immune disease and tumor. This study was conducted following the Declaration of Helsinki, was

approved by the Ethics Review Board of the Affiliated Hospital of Qingdao University (QYFY WZLL 26787), and informed consent was taken from all individual participants.

Clinical analysis of subjects

Data, including age, sex, vital signs (blood pressure and pulse), history (hypertension and diabetes), personal history (smoking and drinking history), and basic laboratory examinations (glucose, triglyceride, total cholesterol, low-density lipoprotein, high-density lipoprotein, white blood cell count, and uric acid), were collected from medical records of all the subjects at the time of registration. All the healthy controls underwent electrocardiography (ECG) and brain imaging examinations (head computed tomography (CT) scan or head MR scan), while the RSSI patients received the following examinations: cerebral MRI, carotid artery examination, and cerebrovascular examination (arterial CTA or MRA), cardiac ultrasound, and 24-h Holter electrocardiogram. A total of 146 RSSI patients completed the head susceptibility-weighted imaging (SWI) examination. RSSI patients underwent laboratory examinations with respect to C-reactive protein, high sensitivity C-reactive protein, and homocysteine. We also evaluated the patients' NIHSS score at admission and 14 days and calculated ΔNIHSS (NIHSS at admission–NIHSS at 14 days) and percentage of NIHSS improvement ((NIHSS at admission–NIHSS at 14 days)/NIHSS at admission). Also, the total MRI burden of patients in the RSSI group was estimated.

Serum analysis for FAM19A5 levels

Fasting blood was withdrawn within 24 h of admission, and the serum was collected by centrifugation at $1,000\times$ g for 15 min and stored at $-80\ °C$. The serum FAM19A5 level of all patients was determined by a double sandwich enzyme-linked immunosorbent assay kit (Jonln Biology, Wuhan, China), with inter-assay CV% < 10%, and intra-assay CV% < 15%, using 50 μL of each sample with no sample dilution. We strictly follow the operating instructions: the standard, specimen, and HRP-conjugate detection antibody were added to the microwells pre-coated with the FAM19A5 capture antibody in sequence. After incubation and washing thoroughly, the color was developed by TMB, and the optical density was measured at 450 nm on a microplate reader (Molecular Devices, San Jose, CA, USA).

Radiological assessment

All RSSI patients were examined using 3.0T MRI, and the images were read and analyzed by two professional neurologists; any differences were resolved through discussion with a third analyst. The volume of cerebral infarction was calculated using the ABC/2 method (*Sims et al., 2009*). Each imaging characteristic of the cSVD (WMH, EPVS, lacune, CMB) was evaluated separately. The lacune of presumed vascular origin has defined as a round or ovoid, subcortical, fluid-filled cavity (signal similar to CSF) between 3 mm and 15 mm in diameter, consistent with a previous acute small subcortical infarct or hemorrhage in the territory of one perforating arteriole. EPVS has defined as fluid-filled spaces that follow the typical course of a vessel as it goes through grey or white matter. The spaces have a signal intensity similar to CSF on all sequences. According to Potter scale, we

counted the number of enlarged perivascular spaces and divided them into 0, 1, 2, 3, and 4 grades (0, 1–10, 11–20, 21–40, ≥40, respectively) (*Potter et al., 2015*). WMH has been defined as a signal abnormality of variable size in the white matter that shows the following characteristics: hyperintensity on T2-weighted images (T2WI) such as fluid-attenuated inversion recovery without cavitation (signal different from CSF); WMH was divided into periventricular WMH (PVWMH) and deep WMH (DWMH) that were graded by Fazekas scale, respectively (*Wardlaw et al., 2013b*), Only RSSI patients with head SWI were evaluated for CMB, which was defined as a small focal round lesion (diameter <10 mm), showing a low signal on SWI. The CMB was classified into lobar CMB and deep CMB. The presence of lacune, the presence of CMB, the number of EPVS ≥11, Fazekas scale ≥2, and each parameter assessed as one score were included in the total MRI burden of cSVD.

Statistical analysis

The normality of quantitative data distribution was assessed using the Kolmogorov–Smirnov test. Continuous variables with normal distribution were described as mean ± standard deviation (SD), continuous variables with non-normal distribution were described as median (interquartile range (IQR)), and qualitative data were described as quantity (percentage). Multivariable logistic regression analysis compared the difference in FAM19A5 expression between the RSSI group and healthy controls, while multivariable linear regression analysis compared the correlation between FAM19A5 and the infarct volume. In order to verify the correlation between the imaging characteristics of total MRI burden and FAM19A5, we first determined the confounding factors by univariate logistic analysis, and those with P-value < 0.1 were included in multivariable logistic analysis for adjustment. Due to the high incidence of WMH and EPVS, the variables were classified into different grades that were analyzed by multivariate ordinal logistic regression. Next, lacune and CMB were analyzed by multivariate binary logistic regression with the classification into the presence and absence. Deep and lobar CMB and, as well as PVWMH and DWMH were independently analyzed by multivariate logistics. $P < 0.05$ was considered statistically significant. In the RSSI group, the correlation between FAM19A5 levels and clinical scales (NIHSS scale at NIHSS scale at admission, NIHSS scale at 14 days, ΔNIHSS, percentage of NIHSS improvement, and total MRI burden of cSVD) were assessed, in which Spearman's test performed the comparisons between continuous variables. All statistical analyses were performed using IBM SPSS Statistics for Windows, version 26.0 (IBM Corporation, Armonk, NY, USA).

RESULTS

Recruitment and baseline characteristics of subjects

A total of 609 subjects were selected in our study from 1784 RSSI patients and healthy individuals from May 2018 to June 2020 (Fig. 1). There were 1,342 acute infarction patients were included in the filter process; among them, 573 patients with severe large artery stenosis and occlusion were excluded, and 188 patients were excluded because of cardiac diseases or other diseases that may lead to cerebral infarctions. Finally, 344 RSSI patients were included in the current study, the mean age was 61.874 ± 11.359 years, and
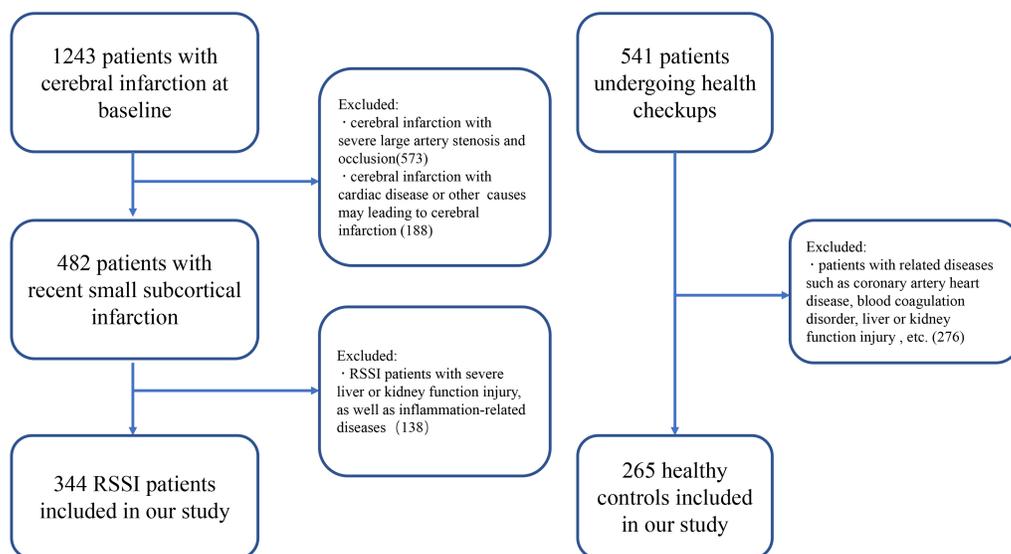
Figure 1 Recruitment flowchart.

Full-size 🖼 DOI: 10.7717/peerj.13101/fig-1

Table 1 Baseline characteristics of RSSI group and healthy controls.

	RSSI ($n = 334$)	Healthy control ($n = 265$)
Age, years (SD)	61.874 ± 11.359	61.411 (11.978)
Sex, male (n%)	211 (63.173)	115 (43.396)
hypertension, n (n%)	207 (61.976)	131 (49.434)
Diabetes, n (n%)	90 (27.245)	44 (16.604)
Current smoking, n (n%)	121 (36.228)	33 (13.415)
Pulse, beats/min (IQR)	68 (59–77)	69 (63–76)
SBP, mmHg (IQR)	151 (137–167)	133 (120–149)
DBP, mmHg (IQR)	84 (76–95)	76 (68–84)
FAM19A5, ng/mL(SD)	0.682 ± 1.225	0.433 ± 0.778

Notes.
SBP, systolic blood pressure; DBP, diastolic blood pressure; FAM19A5, family with sequence similarity 19 memberA5.

211 (63.2%) patients were males. Also, 265 healthy controls were strictly filtered from 541 patients undergoing health checkups, the mean age was 61.411 ± 11.978 years, and 115 (43.4%) patients were males (Table 1).

FAM19A5 level and infarct volume of RSSI

The current study showed a positive correlation between FAM19A5 and recent small subcortical infarct. Mean ± standard deviation of serum FAM19A5 in the RSSI and healthy control groups was 681.894 ± 1225.014 and 432.582 ± 777.871 pg/mL, respectively (Fig. 2). After adjustment for age, sex, hypertension, diabetes, smoking, pulse, triglyceride, cholesterol, low-density lipoprotein, and glucose, our results showed that the expression of FAM19A5 was higher in the RSSI group than the control group (odds ratio (OR) (95% confidence interval (CI)) = 1.265 (1.032–1.549), $P = 0.023$). The linear regression analysis

FAM19A5 levels of RSSI group & healthy control
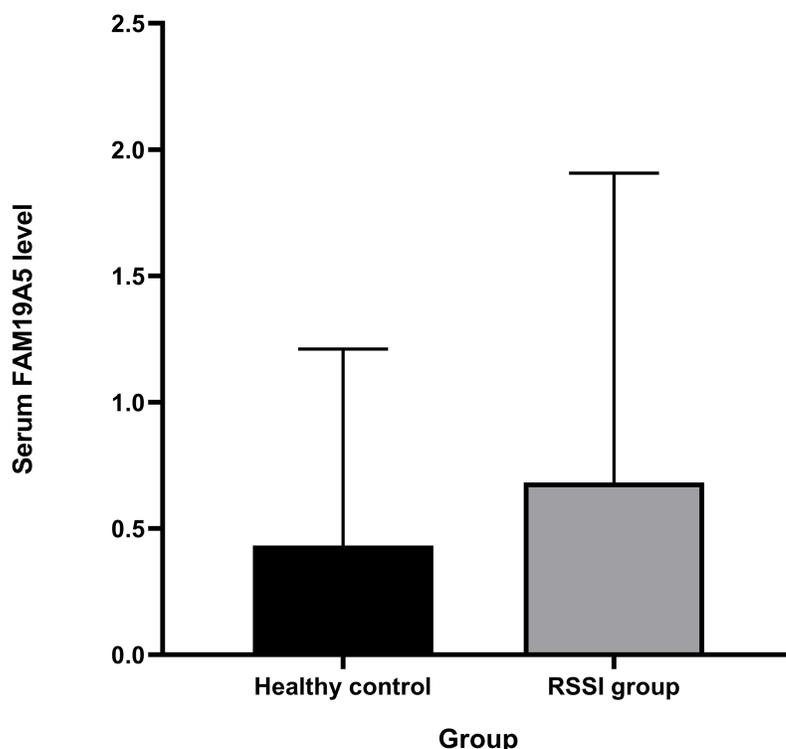
Figure 2 FAM19A5 levels of RSSI group & healthy control. Serum level of FAM19A5 (ng/mL) in the RSSI group (mean $\pm$ SD = 0.682 $\pm$ 1.225) is higher than in healthy control (mean $\pm$ SD = 0.433 $\pm$ 0.778), P-value = 0.023.

Full-size ◨ DOI: 10.7717/peerj.13101/fig-2

of infarct persons showed the correlation between infarct volume and FAM19A5 (OR (95% CI) = 1.587 (1.324–1.901), $P < 0.001$) (Table 2).

FAM19A5 and imaging characteristics of total MRI burden

Serum FAM19A5 levels in imaging characteristics of cSVD total MRI burden are depicted in Fig. 3. A positive correlation between the total MRI burden of cSVD and FAM19A5 levels was established ($P = 0.041$) and assessed by univariate and multivariable regression analysis. (Table 3) Age, sex, hypertension, diabetes, smoking, drinking, pulse, blood pressure, volume of cerebral infarction, glucose, C-reactive protein, triglyceride, total cholesterol, low-density lipoprotein, high-density lipoprotein, white blood cell count, uric acid, and homocysteine were included in the adjustment process.

After adjustment for age, hypertension, pulse, systolic blood pressure, total cholesterol, low-density lipoprotein, C-reactive protein, and high sensitivity C-reactive protein, multivariate ordinal logistic regression analysis showed a positive correlation between FAM9A5 and white matter hypertension on Fazekas scale (OR (95% CI) =1.842 (1.459–2.326), $P < 0.001$). (Table 3) Our further analysis showed that FAM19A5 was correlated

Table 2 Correlation between FAM19A5 and RSSI with its infarct volume.

	Unadjusted		Adjusted[a]	
	OR (95% CI)	*P*-value	OR (95% CI)	*P*-value
Model 1[b]				
RSSI group *vs.* healthy controls	1.029 (1.077–1.559)	**0.006**	1.265 (1.032–1.549)	**0.023**
Model 2[c]				
FAM19A5 and infarct volume	1.597 (1.339–1.906)	**<0.001**	1.587 (1.324–1.901)	**<0.001**

Notes.
[a] Adjusted for age, sex, hypertension, diabetes, current smoking, pulse, triglyceride, cholesterol, lowdensity lipoprotein, glucose.
[b] Binary logistic regression analysis of FAM19A5 level between RSSI group and heathy controls.
[c] Linear regression analysis of FAM19A5 level and infarct volume of RSSI patients. $R^2 = 0.094$. Bold indicates statistically significant *P*-values ($P < 0.05$).

with both periventricular white matter hypertensy (OR (95% CI) = 1.560 (1.311–1.855), $P < 0.001$) and deep white matter hypertensy (OR (95% CI) = 1.557 (1.268–1.910), $P < 0.001$).

After adjustment for age, sex, hypertension, smoking, total cholesterol, and low-density lipoprotein, multivariate ordinal logistic regression analysis showed a positive correlation between FAM9A5 and EPVS Potter scale (OR (95% CI) = 1.434 (1.211–1.698), $P < 0.001$).

The current study did not identify any significant correlation between FAM9A5 and the presence or absence of lacunae (OR (95% CI) = 0.980 (0.801–1.199), $P = 0.844$) and CMB (OR (95% CI) = 0.895 (0.659–1.216), $P = 0.479$). We also found that deep microhemorrhage and cortical microhemorrhage were not related to the FAM19A5 level.

Correlation between FAM19A5 and outcomes

The mean ± SD of NIHSS at admission, NIHSS at 14 days, and ΔNIHSS was 3.22 ± 2.88, 2.52 ± 2.66, and 0.69 ± 1.27, respectively, and the mean ± SD of the percentage of NIHSS improvement was 25.4 ± 48.5. Spearman's correlation analysis demonstrated that the FAM19A5 level was not significantly correlated with NIHSS at admission and 14 days after admission. However, it was positively correlated with ΔNIHSS ($P = 0.031$) and the percentage of NIHSS improvement ($P = 0.011$) (Table 4).

DISCUSSION

The results showed that FAM19A5 increased in the RSSI group, showing a positive correlation with cerebral infarction volume. The multivariate logistic analysis showed that the level of FAM19A5 was positively correlated with the total MRI burden of cSVD, which might be effectuated through the correlation with WMH and EPVS. Moreover, FAM19A5 suggested a better outcome for RSSI patients. By combining the laboratory biomarker with clinical and imaging findings, we verified the association of FAM19A5 with the severity of cSVD and its prognosis, which might guide the treatment of cerebral small vessel diseases.

Reportedly, FAM19A5 participates in nervous system development at an early stage. It is expressed in neurons, oligodendrocyte precursor cells (OPCs), astrocytes, and microglia and is involved in the OPC-mediated repair process as an acute inflammatory factor after pathological brain injury (*Shahapal et al., 2019*). Previous studies have shown that FAM19A5 increases the level of pro-inflammatory cytokines and participates in the
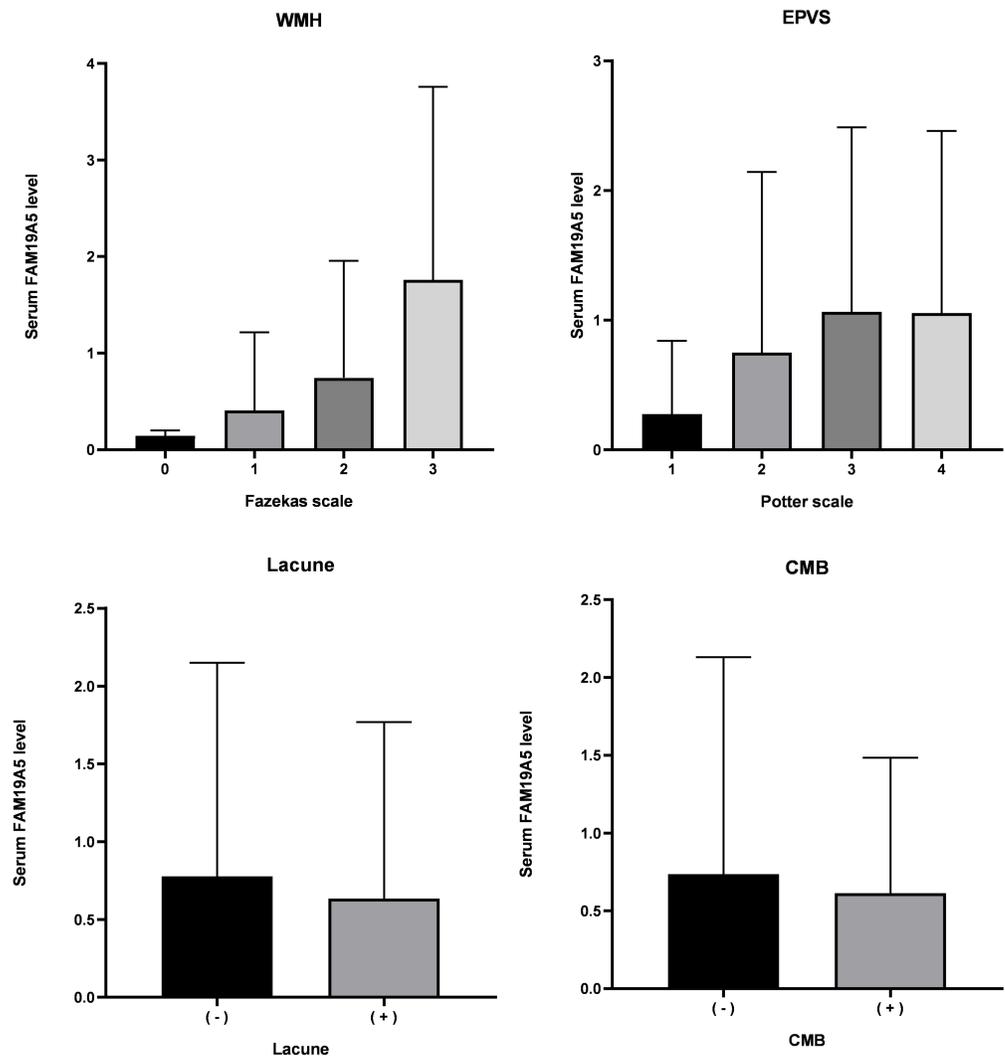
Figure 3 Level of FAM19A5 and imaging characteristics of total MRI burden. FAM19A5 level in persons with Fazekas scale 0, 1, 2, and 3: 0.144 ± 0.056, 0.415 ± 0.814, 0.745 ± 1.211, and 1.761 ± 2.001, respectively. ($n = 4$, 182, 116, and 42, respectively. $P < 0.001$). FAM19A5 level in persons with Potter scale 1, 2, 3, and 4: 0.276 ± 0.564, 0.751 ± 1.392, 1.065 ± 1.423, and 1.0162 ± 1.388, respectively. ($n = 114$, 122, 84, and 24, respectively. $P < 0.001$). FAM19A5 level in persons without or with Lacune: 0.777 ± 1.372 and 0.635 ± 1.134, respectively. ($n = 125$ and 219, $P = 0.844$). FAM19A5 level in persons without or with CMB: 0.736 ± 1.395 and 0.614 ± 0.870, respectively. ($n = 95$ and 51, $P = 0.479$). CMB, cerebral microbleed; EPVS, enlarged perivascular space; WMH, white matter hyperintensity. Bold indicates statistically significant P-values ($P < 0.05$). FAM19A5 level was described as mean $\pm$ standard deviation.

Full-size 🖼 DOI: 10.7717/peerj.13101/fig-3

TNF-α-induced inflammatory response in the hypothalamus, which also confirms the role of FAM19A5 in acute inflammation (*Kang et al., 2020*). A clinical study demonstrated that FAM19A5 was increased in neuromyelitis optica spectrum disorders, the reason may be that after central nervous system (CNS) injury, FAM19A5 is secreted by reactive astrocytes, which triggers excessive proliferation of neuroglial cells and participates in the proliferation of reactive gliosis (*Lee et al., 2019*). Not only acute injury, but also

Table 3 Correlation between FAM19A5 and characteristics of cSVD total MRI burden.

	Unadjusted		Adjusted	
	OR (95% CI)	*P*-value	OR (95% CI)	*P*-value
WMH[a]				
Fazekas scale	1.697 (1.408–2.044)	**<0.001**	1.842 (1.459–2.326)	**<0.001**
EPVS[b]				
Potter scale	1.430 (1.213–1.687)	**<0.001**	1.434 (1.211–1.698)	**<0.001**
Lacune[c]				
Presence or absence	0.913 (0.765–1.89)	0.311	0.980 (0.801–1.199)	0.844
CMB[d]				
Presence or absence	0.917 (0.683–1.232)	0.567	0.895 (0.659–1.216)	0.479
cSVD[e]				
Total MRI burden	1.183 (1.011-1.384)	**0.036**	1.251(1.010-1.550)	**0.041**

Notes.

WMH, EPVS, and total MRI burden underwent ordinal logistic regression, Lacune and CMB were assessed by binary logistic regression.
[a] Adjusted for age, hypertension, pulse, SBP, TC, LDL, CRP, and hsCRP.
[b] Adjusted for age, sex, hypertension, smoking, TC, and LDL.
[c] Adjusted for age, hypertension, SBP, and Hcy.
[d] Adjusted for glucose, TC, and UA.
[e] Adjusted for age, SBP, glucose, TC, LDL, CRP, and Hcy.
SBP, systolic blood pressure; TC, total cholesterol; LDL, low-density lipoprotein; Hcy, homocysteine; CI volume, cerebral infarction volume; CRP, C-reactive protein; hsCRP, high sensitivity C-reactive protein.
Bold indicates statistically significant *P*-values ($P < 0.05$).

Table 4 Association of FAM19A5 levels with clinical scales of patients.

	RSSI ($n = 334$)	*P*-value
NIHSS scale at admission	3.2173 ± 2.881	0.869
NIHSS scale at 14 days	2.524 ± 2.657	0.109
ΔNIHSS	0.693 ± 1.269	**0.031**
Percentage of NIHSS improvement, %	25.361 ± 48.454	**0.011**

Notes.

NIHSS, National Institutes of Health stroke scale.
Bold indicates statistically significant *P*-values ($P < 0.05$).

FAM19A5 is involved in the pathophysiological process of chronic inflammation. As a bridge connecting chronic inflammation, reactive gliosis, and degenerative diseases in the brain, FAM19A5 is overexpressed in severe depressive disorder and negatively correlated with cortical thickness. It is also highly expressed in Alzheimer's in genetic studies and vascular dementia (*Han et al., 2020*; *Li et al., 2020*; *Mez et al., 2017*).

Microglia and astrocytes are activated in acute infarction, leading to high expression of inflammatory factors *via* damage-associated molecular pattern (DAMPs) and "inflammatory waterfall" however, the correlation between FAM19A5 and RSSI has not yet been realized (*Chen & Nuñez, 2010*). To the best of our knowledge, we assessed the expression of FAM19A5 in cSVD and found that the expression level of FAM19A5 in RSSI patients was high and correlated with the infarct volume of RSSI. Based on the previous studies, we speculated that the reasons for the increased expression of FAM19A5 after cerebral infarction might be as follows: FAM19A5 is secreted by reactive glial cells

and is involved in OPC-mediated repair process, triggers glial cell proliferation, and glial scar formation. This phenomenon is confirmed by the correlation between FAM19A5 and cerebral infarction volume: a large volume of brain injury indicates severe nerve damage and acute inflammation. Also, higher FAM19A5 predicted a larger ΔNIHSS and percentage of NIHSS improvement, suggesting that FAM19A5 contributes to the repair process of the nervous system *via* OPC-mediated gliosis and nerve repair process, thereby improving the stroke prognosis.

The mechanism of cerebral small vessel disease is complex, and the pathogenesis varies in imaging characteristics of cSVD and in different areas of the brain (*Blanco, Müller & Spence, 2017*). Deep CMB is closely related to hypertension, and lobar CMB might be caused by cerebral vascular amyloidosis (*Ding et al., 2015*; *Poels et al., 2010*; *Wardlaw, Smith & Dichgans, 2013a*). Several studies have shown that high signal intensity in white matter is correlated with the overexpression of various inflammatory factors (*Satizabal et al., 2012*). The disturbance of cerebrospinal fluid circulation in perivascular space or the imbalance of aquaporin in astrocytes might be one of the causes of EPVS. In addition, histopathological studies have shown that PVS is consistent with the location of inflammatory infiltration in EPVS (*Kwee & Kwee, 2007*). Lacune is usually considered to be transformed from other lesions (*Wardlaw, Smith & Dichgans, 2013a*; *Wardlaw, Smith & Dichgans, 2019*). Our correlation analysis results suggested that higher FAM19A5 levels reflect a severe total MRI burden, and multivariate logistic analysis showed that FAM19A5 reflects the severity of WMH and EPVS. Comprehensively, we speculated that the correlation between FAM19A5 and total MRI burden could be attributed to the effects on WMH and EPVS, which might be due to the involvement of FAM19A5 in chronic inflammation in the brain. Since WMH and EPVS are related to chronic and persistent inflammatory responses, the expression and activity of many inflammatory markers are elevated (*Blanco, Müller & Spence, 2017*; *Kwee & Kwee, 2007*; *Satizabal et al., 2012*). Herein, we did not find any correlation between deep or lobar CMB and FAM19A5. Comprehensively, the reason may be that CMBs are related to hypertension or amyloidosis, reflecting the deposition of hemosiderin in macrophages and failing to reflect the persistent inflammatory response of the brain (*Janaway et al., 2014*). In addition, lacunae are usually thought to be transformed from other lesions, and it is complex to trace encephalomalacia to its origins. Therefore, the etiology and mechanism are complex and lack solid evidence. Taken together, FAM19A5 is used as a chronic inflammatory factor that participates in the progression of cSVD and reflects its severity.

Nevertheless, the present study has several limitations. Firstly, because of our strict screening of patients with cerebral infarction, the study included only a small number of cases, and the various examination strategies of subcenters refer to insufficient tests in SWI examinations, thereby limiting the CMB research. Secondly, our subjects are homogeneous, and most of them are Han people in northern China. This problem could be solved by increasing the number of patients in the future. Thirdly, severe large artery stenosis was defined as stenosis >50% of a carotid or intracranial artery according to TOAST, it is the most broadly used but may leading to the insufficient exclusion of those with a high carotid plaque burden. Other classification systems like SPARKLE and CISS is meaningful

in solving this problem in the future.(*Bogiatzi et al., 2014*; *Zhang et al., 2019*) Finally, due to the limitations of the cross-sectional analysis, we are unable to study causality. Thus, additional studies and dynamic observation are needed to solve this problem in the future.

In summary, FAM19A5 reflects the severity of RSSI and predicts a promising prognosis as an acute inflammatory factor. In the imaging characteristics of cSVD, FAM19A5 can reflect the severity of WMH and EPVS. That might guide the diagnosis and treatment of cerebrovascular diseases.

ACKNOWLEDGEMENTS

ADDITIONAL INFORMATION AND DECLARATIONS

Funding

Grant Disclosures

Competing Interests

The authors declare there are no competing interests.

Author Contributions

- Zhongnan Hao conceived and designed the experiments, performed the experiments, analyzed the data, prepared figures and/or tables, authored or reviewed drafts of the paper, and approved the final draft.
- Shaonan Yang, Ruihua Yin and Yuan Wang analyzed the data, prepared figures and/or tables, authored or reviewed drafts of the paper, and approved the final draft.
- Jin Wei performed the experiments, prepared figures and/or tables, authored or reviewed drafts of the paper, and approved the final draft.
- Xudong Pan and Aijun Ma conceived and designed the experiments, authored or reviewed drafts of the paper, and approved the final draft.

Human Ethics

The following information was supplied relating to ethical approvals (i.e., approving body and any reference numbers):

The Ethics Review Board of the Affiliated Hospital of Qingdao University

Data Availability

The following information was supplied regarding data availability:

The raw measurements are available in the Supplementary File.

Supplemental Information

Supplemental information for this article can be found online at http://dx.doi.org/10.7717/peerj.13101#supplemental-information.

REFERENCES

Blanco PJ, Müller LO, Spence JD. 2017. Blood pressure gradients in cerebral arteries: a clue to pathogenesis of cerebral small vessel disease. *Stroke and Vascular Neurology* **2**:108–117 DOI 10.1136/svn-2017-000087.

Bogiatzi C, Wannarong T, McLeod AI, Heisel M, Hackam D, Spence JD. 2014. SPARKLE (Subtypes of Ischaemic Stroke Classification System), incorporating measurement of carotid plaque burden: a new validated tool for the classification of ischemic stroke subtypes. *Neuroepidemiology* **42**:243–251 DOI 10.1159/000362417.

Cannistraro RJ, Badi M, Eidelman BH, Dickson DW, Middlebrooks EH, Meschia JF. 2019. CNS small vessel disease: a clinical review. *Neurology* **92**:1146–1156 DOI 10.1212/WNL.0000000000007654.

Chen GY, Nuñez G. 2010. Sterile inflammation: sensing and reacting to damage. *Nature Reviews Immunology* **10**:826–837 DOI 10.1038/nri2873.

Ding J, Sigurdsson S, Garcia M, Phillips CL, Eiriksdottir G, Gudnason V, Van Buchem MA, Launer LJ. 2015. Risk factors associated with incident cerebral microbleeds according to location in older people: the age, gene/environment susceptibility (AGES)-Reykjavik study. *JAMA Neurology* **72**:682–688 DOI 10.1001/jamaneurol.2015.0174.

Gattringer T, Eppinger S, Pinter D, Pirpamer L, Berghold A, Wünsch G, Ropele S, Wardlaw JM, Enzinger C, Fazekas F. 2015. Morphological MRI characteristics of recent small subcortical infarcts. *International Journal of Stroke: Official Journal of the International Stroke Society* **10**:1037–1043 DOI 10.1111/ijs.12499.

Han K-M, Tae W-S, Kim A, Kang Y, Kang W, Kang J, Kim Y-K, Kim B, Seong JY, Ham B-J. 2020. Serum FAM19A5 levels: a novel biomarker for neuroinflammation and neurodegeneration in major depressive disorder. *Brain, Behavior, and Immunity* **87**:852–859 DOI 10.1016/j.bbi.2020.03.021.

Janaway BM, Simpson JE, Hoggard N, Highley JR, Forster G, Drew D, Gebril OH, Matthews FE, Brayne C, Wharton SB, Ince PG, Function MRCC, Ageing Neuropathology S. 2014. Brain haemosiderin in older people: pathological evidence for an ischaemic origin of magnetic resonance imaging (MRI) microbleeds. *Neuropathology and Applied Neurobiology* **40**:258–269 DOI 10.1111/nan.12062.

Kang D, Kim HR, Kim KK, Kim DH, Jeong B, Jin S, Park JW, Seong JY, Lee BJ. 2020. Brain-specific chemokine FAM19A5 induces hypothalamic inflammation. *Biochemical and Biophysical Research Communications* **523**:829–834 DOI 10.1016/j.bbrc.2019.12.119.

Kwee RM, Kwee TC. 2007. Virchow-Robin spaces at MR imaging. *Radiographics: A Review Publication of the Radiological Society of North America, Inc* **27**:1071–1086 DOI 10.1148/rg.274065722.

Lee HL, Seok HY, Ryu H-W, Cho EB, Kim BC, Kim BJ, Min J-H, Seok JM, Shin HY, Kang S-Y, Kwon O-H, Lee S-S, Oh J, Sohn E-H, Huh S-Y, Cho J-Y, Seong JY, Kim B-J. 2019. Serum FAM19A5 in neuromyelitis optica spectrum disorders: can it be a new biomarker representing clinical status? *Multiple Sclerosis (Houndmills, Basingstoke, England)* 1352458519885489 DOI 10.1177/1352458519885489.

Li XN, Hao DP, Qu MJ, Zhang M, Ma AB, Pan XD, Ma AJ. 2021. Development and Validation of a Plasma FAM19A5 and MRI-Based Radiomics Model for Prediction of Parkinson's Disease and Parkinson's Disease With Depression. *Frontiers in Neuroscience* 15:795539 DOI 10.3389/fnins.2021.795539.

Li J, Li S, Song Y, Zhou W, Zhu X, Xu S, Ma Y, Zhu C. 2020. Association of serum FAM19A5 with cognitive impairment in vascular dementia. *Disease Markers* 2020:8895900 DOI 10.1155/2020/8895900.

Mez J, Chung J, Jun G, Kriegel J, Bourlas AP, Sherva R, Logue MW, Barnes LL, Bennett DA, Buxbaum JD, Byrd GS, Crane PK, Ertekin-Taner N, Evans D, Fallin MD, Foroud T, Goate A, Graff-Radford NR, Hall KS, Kamboh MI, Kukull WA, Larson EB, Manly JJ, Haines JL, Mayeux R, Pericak-Vance MA, Schellenberg GD, Lunetta KL, Farrer LA. 2017. Two novel loci, COBL and SLC10A2, for Alzheimer's disease in African Americans. *Alzheimers Dement* 13:119–129 DOI 10.1016/j.jalz.2016.09.002.

Poels MMF, Vernooij MW, Ikram MA, Hofman A, Krestin GP, van der Lugt A, Breteler MMB. 2010. Prevalence and risk factors of cerebral microbleeds: an update of the Rotterdam scan study. *Stroke* 41:S103–S106 DOI 10.1161/STROKEAHA.110.595181.

Potter GM, Chappell FM, Morris Z, Wardlaw JM. 2015. Cerebral perivascular spaces visible on magnetic resonance imaging: development of a qualitative rating scale and its observer reliability. *Cerebrovascular Diseases (Basel, Switzerland)* 39:224–231 DOI 10.1159/000375153.

Satizabal CL, Zhu YC, Mazoyer B, Dufouil C, Tzourio C. 2012. Circulating IL-6 and CRP are associated with MRI findings in the elderly: the 3C-Dijon Study. *Neurology* 78:720–727 DOI 10.1212/WNL.0b013e318248e50f.

Shahapal A, Cho E, Yong H, Jeong I, Kwak H, Lee J, Kim W, Kim B, Park H, Lee W, Kim H, Hwang J, Seong J. 2019. FAM19A5-LacZFAM19A5 expression during embryogenesis and in the adult traumatic brain of knock-in mice. *Frontiers in Neuroscience* 13:917 DOI 10.3389/fnins.2019.00917.

Sims JR, Gharai LR, Schaefer PW, Vangel M, Rosenthal ES, Lev MH, Schwamm LH. 2009. ABC/2 for rapid clinical estimate of infarct, perfusion, and mismatch volumes. *Neurology* 72:2104–2110 DOI 10.1212/WNL.0b013e3181aa5329.

Tom Tang Y, Emtage P, Funk WD, Hu T, Arterburn M, Park EEJ, Rupp F. 2004. TAFA: a novel secreted family with conserved cysteine residues and restricted expression in the brain. *Genomics* 83:727–734 DOI 10.1016/j.ygeno.2003.10.006.

Wardlaw JM, Smith C, Dichgans M. 2013a. Mechanisms of sporadic cerebral small vessel disease: insights from neuroimaging. *The Lancet Neurology* 12:483–497 DOI 10.1016/S1474-4422(13)70060-7.

Wardlaw JM, Smith C, Dichgans M. 2019. Small vessel disease: mechanisms and clinical implications. *The Lancet Neurology* 18:684–696 DOI 10.1016/S1474-4422(19)30079-1.

Wardlaw JM, Smith EE, Biessels GJ, Cordonnier C, Fazekas F, Frayne R, Lindley RI, O'Brien JT, Barkhof F, Benavente OR, Black SE, Brayne C, Breteler M, Chabriat H, Decarli C, De Leeuw F-E, Doubal F, Duering M, Fox NC, Greenberg S, Hachinski V, Kilimann I, Mok V, Oostenbrugge Rv, Pantoni L, Speck O, Stephan BCM, Teipel S, Viswanathan A, Werring D, Chen C, Smith C, Van Buchem M, Norrving B, Gorelick PB, Dichgans M. 2013b. Neuroimaging standards for research into small vessel disease and its contribution to ageing and neurodegeneration. *The Lancet Neurology* **12**:822–838 DOI 10.1016/S1474-4422(13)70124-8.

Zhang H, Li Z, Dai Y, Guo E, Zhang C, Wang Y. 2019. Ischaemic stroke etiological classification system: the agreement analysis of CISS. *SPARKLE and TOAST* **4**:123–128 DOI 10.1136/svn-2018-000226.